ELSEVIER

Coastal Engineering 41 (2000) 413–431

COASTAL ENGINEERING

www.elsevier.com/locate/coastaleng

Experimental determination of wavelengths in the presence of a mean current

Richard R. Simons *, Ruairi D. MacIver

Department of Civil and Environmental Engineering, University College of London, Gower Street, London WC1E 6BT, UK

Received 1 June 1999; received in revised form 29 February 2000; accepted 22 March 2000

Abstract

This paper describes a simple method for determining the wavelength of small amplitude waves under laboratory conditions where reflected wave components are present both with and without a mean current flow superimposed. It assumes a locally horizontal bed but requires no a priori assumption concerning the form of the dispersion relation with a coexisting current. Synchronous measurements of the water surface recorded along any straight line are analysed to yield Fourier coefficients at each location. It is then shown that for all practical conditions excluding a perfect standing wave, the average rate of change of wave phase in the chosen direction can be related directly to the component of incident wave number in that direction, irrespective of reflection coefficient or relative current strength. The technique has been applied to regular and bichromatic waves in a flume with an absorbing wave generator, and can also be applied in 3-D wave basins where waves and currents intersect at arbitrary angles. In combined wave–current experiments, by assuming the linear dispersion relation, it is also possible to estimate the effective current velocity.

Keywords: Waves; Wavelength; Reflection coefficient; Wave phase slope; Wave–current interaction

1. Introduction

All theories that set out to describe water wave motion include a term for the horizontal distance over which the wave form repeats itself in the direction of wave

* Corresponding author. Tel.: +44-20-7679-7723.

E-mail addresses: r.rsimons@ucl.ac.uk (R.R. Simons), r.maciver@ucl.ac.uk (R.D. MacIver).

0378-3839/00/$ - see front matter
PII: S0378-3839(00)00039-9

Nomenclature:

A_x	amplitude of partial standing wave at location x
a_1	awave amplitude of incident wave
a_2	wave amplitude of reflected wave
h	mean water depth
L_1	wavelength of incident wave
L_2	wavelength of reflected wave
L_R	modulation length of wave amplitude along the flume $= 2\pi/(m_1 + m_2) = L_1 L_2/(L_2 + L_2)$
m_1	wave number for incident wave
m_2	wave number for reflected wave
t	time
T	wave period
U_c	effective mean current superimposed onto the waves
U_{c1}	effective mean current calculated from observed incident wavelength
x	horizontal coordinate (positive in the direction of mean current flow)
z	vertical coordinate (positive up from still water level)
α_r	reflection coefficient (as fraction)
Δm	difference between incident wave number and average rate of change of phase in the direction of wave propagation
η	time-varying wave surface elevation
ϕ	phase shift between reflected and incident waves at $x = 0$
ϕ_x	phase of partial standing wave at location x
θ	spatial phase angle
ω	angular wave frequency

propagation. This is true whether or not the theory attempts to include the effects of wave–current interaction. The accurate measurement of wavelength thus forms an important stage in the validation of any wave theory.

Even for the simplest of wave experiments, where a train of regular long-crested waves propagates along an infinite flume with no reflection or mean current flowing, the measurement of wavelength requires some care. Using surface-touching pointers, two such devices have to be moved apart along the line of wave propagation such that they are both, simultaneously and momentarily, just wetted by the passage of two consecutive wave crests. The probes are then one wavelength apart. However, the difficulty of identifying the point at which both probes are simultaneously wetted makes the approach susceptible to large errors. This problem can be reduced by the use of resistance-type wave probes to measure the water surface profiles at two locations along the flume, synchronising the signals from the two probes by gradually sliding them apart. This method works well, but can again lead to significant error, for instance, when the water surface is modulated by reflected or free second-harmonic waves.

With the advent of random wave generators in hydraulics laboratories, Thornton and Calhoun (1972) and subsequently Goda and Suzuki (1976) proposed methods to identify both the incident and reflected wave characteristics at each frequency component in a wave spectrum. Measurements of surface elevation at two locations, a known distance apart were decomposed into Fourier series, and hence, amplitude and phase for incident and reflected wave at each frequency component. Seelig (1979) extended this with the use of three probes, and Mansard and Funke (1980) presented a least-squares method for identifying incident and reflected wave components based on a similar three-probe deployment. Zelt and Skjelbreia (1992) adopted a weighted least-squares technique to analyse data from an arbitrary number of probes. In a useful review of the topic, Hughes (1993) noted that the effective frequency range for these methods is extended by the use of synchronous data from three unequally-spaced probes. Most laboratory measurements of irregular waves are now performed using co-linear multi-probe arrays with spacings as suggested by Goda, and adopt similar forms of analysis.

All the methods cited above assume, first, that the waves are propagating over a locally flat bottom, secondly, that the dispersion relation from linear wave theory is valid, and thirdly, that the celerities of incident and reflected wave components are the same. However, if a significant mean flow exists, either as a superimposed current flow or through wave-induced mass transport, the wave celerity experiences a Doppler shift. This results in the incident and reflected wave components propagating with measurably different wavelengths. Skyner and Easson (1998) calculated wavelengths in combined wave–current flows using a two-probe method as described above together with photography of the wave elevation. However, their experiments were limited to regular waves, and they avoided the complications introduced by the reflected waves by restricting measurements to the first few incident waves, before the reflections arrived at the test section from the beach.

The present work arose from an investigation into the non-linear effects of wave–current interaction using both regular and irregular wave sequences. Accurate measurements were required of incident wave heights and wavelengths irrespective of the strength or vertical distribution of the mean current flowing. It was thus not appropriate to adopt any method of measurement and analysis that required initial assumptions to be made concerning the dispersion relation and possible Doppler shift, as determination of the effective current strength in the combined wave–current flow was an intended outcome of the research. The section below describes how a method was developed to satisfy these constraints.

2. Theory for 2-D waves

For a wave of period T and length L propagating in the positive x direction on still water of constant depth with no loss of energy, small amplitude wave theory describes the surface displacement as:

$$\eta = a\cos(mx - \omega t) \tag{1}$$

where η is the surface elevation, a is the wave amplitude (generally a function of x), $m = 2\pi/L$ is the wave number, $\omega = 2\pi/T$, and $mx - \omega t$ is the wave phase.

In the absence of reflections and attenuation, wave amplitude is constant. It is also clear that keeping t constant, the phase of such a wave increases linearly in the direction of wave propagation at a constant rate m. Fourier analysis of water surface measurements made at regular intervals in the direction of wave propagation can then be used to determine the rate of change of phase with distance, and hence, the wave number m. This is demonstrated in Fig. 1 for a wave propagating in the negative x direction.

If reflected waves (of the same frequency) propagating in the opposite direction are superimposed on the incident waves, the phase ceases to increase monotonically but now varies periodically in space, Fig. 2; and if a mean current is introduced (such as in experiments investigating wave–current interaction), the situation is further complicated by the reflected waves having a different wavelength from that of the incident waves, Fig. 3. It is for such a combination that the method developed here is intended.

It is assumed initially that the current is steady and uniform over depth and in the propagation direction, and that reflection coefficients are less than 0.41; however, it will be shown later that excellent results can be obtained for all practical reflection

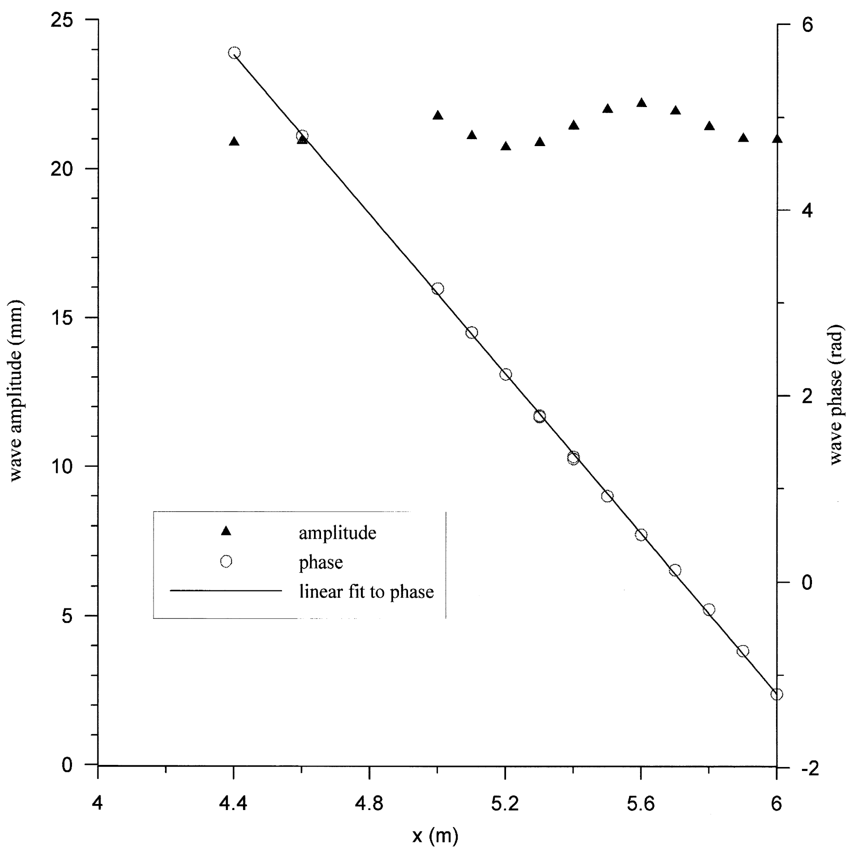

Fig. 1. Wave amplitude and phase along the flume: $T = 1.0$ s (10wr030), $h = 0.4$ m, no current.

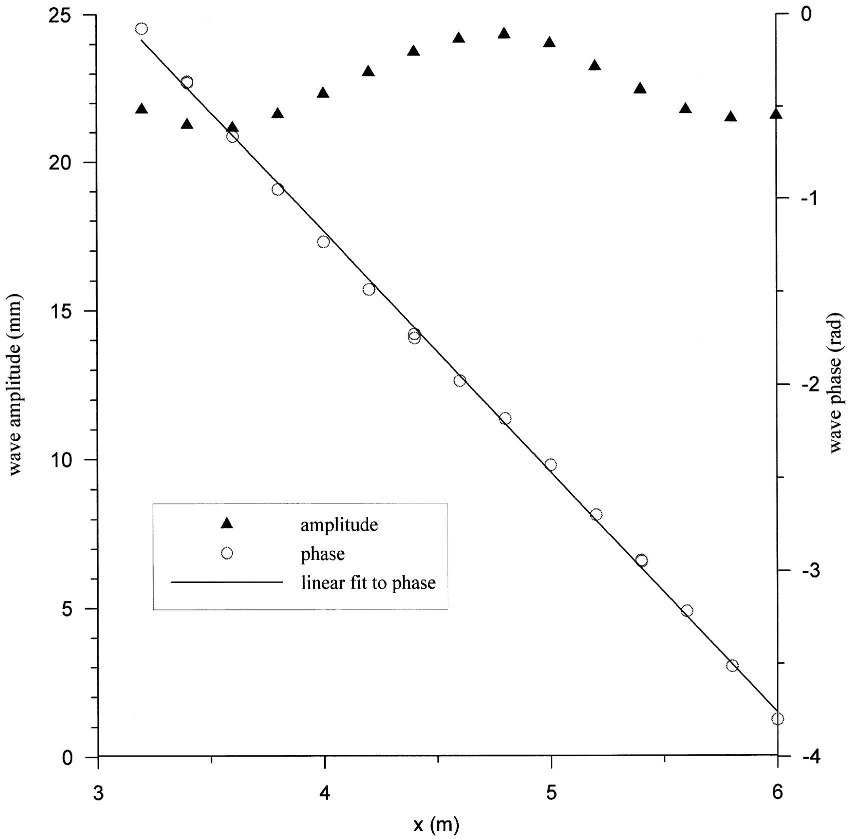

Fig. 2. Wave amplitude and phase along the flume: $T = 2.5$ s (25wr021), $h = 0.4$ m, no current.

coefficients up to a full standing wave and that the method is insensitive to vertical shear in the current.

The water surface for the combined flow can be described by the expression:

$$\eta = a_1\cos(m_1 x - \omega t) + a_2\cos(m_2 x + \omega t + \phi) \tag{2}$$

where $m_1 = 2\pi/L_1$ is the wave number of the incident wave, $m_2 = 2\pi/L_2$ is the wave number of the reflected wave, ω is the angular frequency, a_1 is the amplitude of the incident wave, a_2 is the amplitude of the reflected wave, and ϕ is the phase shift between reflected and incident waves at $x = 0$.

This can be expanded by standard trigonometry to give:

$$\eta = a_1\cos(m_1 x)\cos(\omega t) + a_1\sin(m_1 x)\sin(\omega t) + a_2\cos(m_2 x + \phi)\cos(\omega t) - a_2\sin(m_2 x + \phi)\sin(\omega t) \tag{3}$$

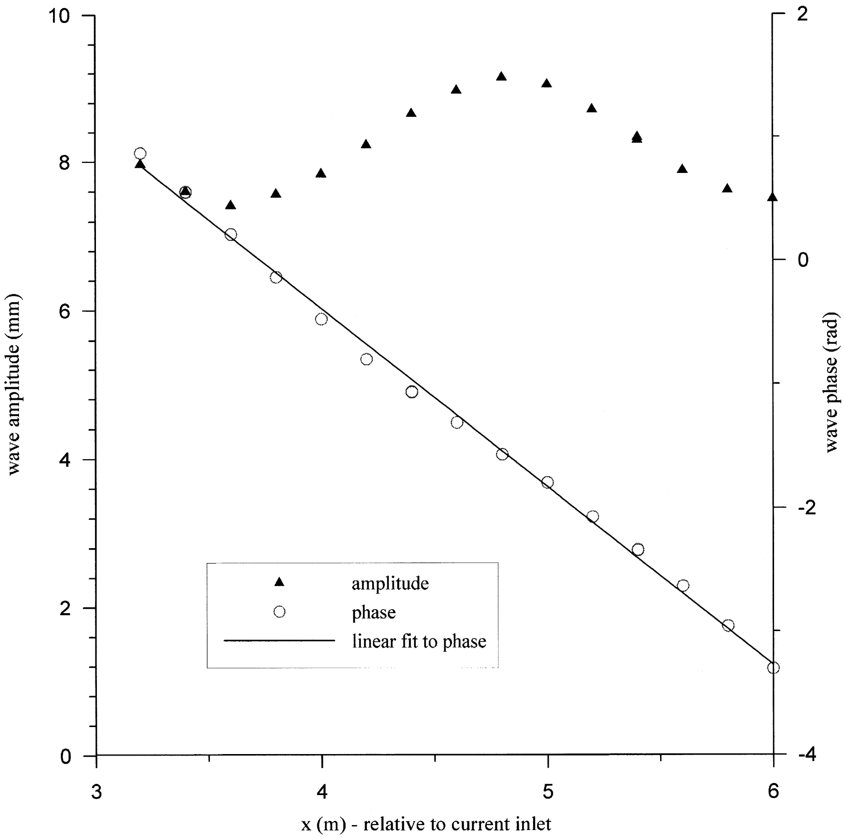

Fig. 3. Wave amplitude and phase along the flume: $T = 2.5$ s (25wf007), $h = 0.4$ m, opposing current.

which, in turn, can be expressed in the form:

$$\eta = A_x \cos(\omega t + \phi_x) \tag{4}$$

where the amplitude and phase are given by:

$$A_x = \sqrt{a_1^2 + a_2^2 + 2a_1 a_2 \cos(m_1 x + m_2 x + \phi)} \tag{4a}$$

$$\phi_x = \arctan\left[\frac{a_1 \sin(m_1 x) - a_2 \sin(m_2 x + \phi)}{a_1 \cos(m_1 x) + a_2 \cos(m_2 x + \phi)}\right]. \tag{4b}$$

In the absence of a reflected wave, $a_2 = 0$ and the rate of change of phase in the direction of wave propagation $\mathrm{d}\phi_x/\mathrm{d}x$ is simply the incident wave number m_1. Following the same approach in the presence of a reflected wave, differentiating Eq. (4b) with respect to x gives:

$$\frac{\mathrm{d}\phi_x}{\mathrm{d}x} = \frac{m_1(a_1^2 + a_1 a_2 \cos(m_1 x + m_2 x + \phi)) - m_2(a_2^2 + a_1 a_2 \cos(m_1 x + m_2 x + \phi))}{a_1^2 + a_2^2 + 2a_1 a_2 \cos(m_1 x + m_2 x + \phi)} \tag{5}$$

which can be re-expressed, exactly, in the form:

$$\frac{\mathrm{d}\phi_x}{\mathrm{d}x} = m_1 - \frac{\left(a_2^2 + a_1 a_2 \cos(m_1 x + m_2 x + \phi)\right)}{a_1^2 + a_2^2 + 2a_1 a_2 \cos(m_1 x + m_2 x + \phi)}(m_1 + m_2). \tag{6}$$

Introducing $\alpha_r = a_2/a_1$, the reflection coefficient expressed as a fraction, and $\theta = [(m_1 + m_2)x + \phi]$, the spatial phase angle, this becomes:

$$\frac{\mathrm{d}\phi_x}{\mathrm{d}x} = m_1 - \frac{\left(\alpha_r^2 + \alpha_r \cos(\theta)\right)}{1 + \alpha_r^2 + 2\alpha_r \cos(\theta)}(m_1 + m_2) = m_1 - \Delta m(x, \alpha_r). \tag{7}$$

Clearly, the reflected wave is modulating the rate of change of spatial wave phase about the incident wave number by an amount Δm which varies with horizontal location x and with reflection coefficient α_r.

If $\alpha_r^2 + 2\alpha_r \cos(\theta) < 1$ (that is: $\alpha_r < 0.414$), the modulation Δm in Eq. (7) can then be developed in the form:

$$\Delta m(x) = (m_1 + m_2)\left[\alpha_r^2 + \alpha_r \cos(\theta)\right]\left[1 + \alpha_r^2 + 2\alpha_r \cos(\theta)\right]^{-1} \tag{8}$$

$$\begin{aligned}\Delta m(x) = (m_1 + m_2)\left[\alpha_r^2 + \alpha_r \cos(\theta)\right]\Big[1 &- \left(\alpha_r^2 + 2\alpha_r \cos(\theta)\right) \\ &+ \left(\alpha_r^4 + 4\alpha_r^3 \cos(\theta) + 4\alpha_r^2 \cos^2(\theta)\right) - \left(\alpha_r^6 + 6\alpha_r^5 \cos(\theta)\right. \\ &\left.+ 12\alpha_r^4 \cos^2(\theta) + 8\alpha_r^3 \cos^3(\theta)\right) + \dots\Big]\end{aligned} \tag{8a}$$

$$\begin{aligned}\Delta m(x) = (m_1 + m_2)\Big[\alpha_r \cos(\theta) &+ \alpha_r^2\left(1 - 2\cos^2(\theta)\right) + \alpha_r^3\left(4\cos^3(\theta)\right. \\ &\left.- 3\cos(\theta)\right) + \alpha_r^4 (8\cos^2(\theta) - 1 - 8\cos^4(\theta) + \dots\Big].\end{aligned} \tag{8b}$$

Simplifying this using standard trigonometric relationships:

$$\Delta m(x) = (m_1 + m_2)\left[\alpha_r \cos(\theta) - \alpha_r^2 \cos(2\theta)) + \alpha_r^3(\cos(3\theta)) - \dots\dots\right] \tag{9}$$

revealing the modulation to be periodic with a fundamental length scale $L_R = L_1 L_2/(L_1 + L_2)$. Averaging the wave phase slope over this modulation length will recover the incident wave number exactly.

This confirms that it is valid to use the *average* rate of change of wave phase over the modulation length L_R in the direction of wave propagation as a reliable measure of incident wave number. However, it is important that the average is determined over the exact modulation length, as $\mathrm{d}\phi/\mathrm{d}x$ does vary significantly with x even with relatively small reflection coefficients (see Fig. 2), and the average over any length not equal to L_R may produce a significantly different estimate of m_1. The procedure thus requires some iteration in the determination of L_1 and L_2 using updated values of L_R. This process is described later.

The linearised Doppler-shifted dispersion relation for waves propagating on a current with an effective mean velocity U_c is:

$$(\omega - mU_c)^2 = gm\tanh(mh). \tag{10}$$

Having determined the incident wave number m_1 from the method described above, the effective mean current, U_{c1}, causing the change in incident wave celerity can be calculated by re-arranging Eq. (10):

$$U_{c1} = \frac{\omega}{m_1} - \sqrt{\frac{g}{m_1}\tanh(m_1 h)}. \tag{11}$$

Assuming that the reflected wave feels an effective mean current equal in magnitude but opposite in direction to that acting on the incident wave (implicitly neglecting the effects of vertical variation in the mean current), the wave number of the reflected wave m_2 can be determined by the iterative solution of a modified Eq. (10):

$$(\omega + m_2 U_{c1})^2 = gm_2\tanh(m_2 h). \tag{12}$$

If the vertical distribution of mean current is known to be non-uniform, an alternative approach is to determine m_2 from the modulation in wave amplitude produced by the reflected wave. Eq. (4a) showed that L_R is the spatial modulation length of the water surface amplitude as well as of the phase, and it can thus be calculated from the wavelength of a best-fit sinusoid through the wave height amplitude modulation along the flume. This technique depends on data being available over a number of incident wavelengths, and on wave attenuation over the test region being negligible.

3. Experiments

The experiments were performed in a glass-walled flume, 0.457 m wide and 16 m long, with a still water depth of 0.4 m (Fig. 4). The layout was similar to but smaller

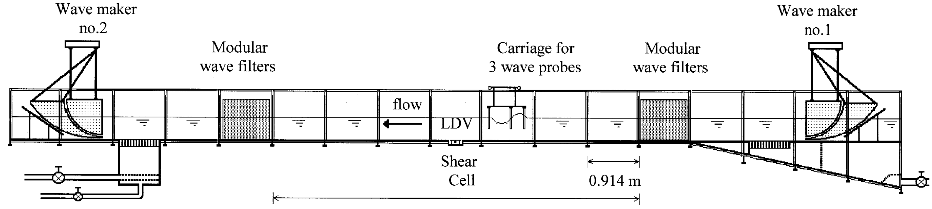

Fig. 4. Side view of UCL wave–current laboratory flume.

than that used by Klopman (1994) for experiments involving waves propagating both with and against a current. The bed was roughened with 6-mm square-section slats placed across the line of wave propagation at 25 mm centres.

Two force-sensitive active-absorption wave makers were installed one at either end of the flume. When in use, one wave maker acted as a wave generator, the other acted as a wave absorber. The wave makers were of a rotating sector design; this produces a piston-type motion at the front face while the back face rotates smoothly along an arc eliminating the generation of back waves. The active absorption system was designed to reduce reflections in the flume, in particular for low frequency components that are notoriously difficult to suppress by traditional means in a relatively short laboratory facility.

However, preliminary tests revealed that the feedback system was unable to reduce reflections to acceptable levels for the higher frequency waves (greater than 0.75 Hz); for these tests, a removable “beach” was installed at the absorption end of the flume. This beach consisted of a thin sheet of perforated metal, 2 m long and 0.455 m wide, suspended horizontally 0.1 m below still water level close to the absorbing wave maker. Kemp and Simons (1983) deployed a similar device and found that it was able to absorb short wave energy while causing minimal interference to the inflow and exit conditions of the mean current. The combination of absorbing wave makers and horizontal beach were found to produce reflection coefficients of between 1.2% and 6% over a wide range of wave frequencies (0.3 to 1.25 Hz), which was particularly relevant for a parallel series of tests propagating random waves on a current.

Each wave maker was driven by a brushless motor, with control signals for wave generation produced by proprietary software supplied by the manufacturers. This gave considerable flexibility in the form of wave generated, and allowed components to be added to the drive signal to suppress spurious free harmonics. In the test programme described here, regular and bichromatic wave sequences were generated.

Currents were driven by a recirculation system fed by a header tank 20 m above the flume. Inlet flow rates were adjusted by a gate valve, while outflow was adjusted using two spear valves to produce the desired water depth midway along the flume. The flow was introduced through the bed of the flume downstream from one of the absorbing wave makers, and was removed through the bed in front of the other. This allowed good symmetry when comparing results from tests on waves with following and opposing currents.

Modular wave filters were installed at both ends of the flume. These had two purposes: first, they removed small cross-waves generated by leakage at the sides of the wave maker units; secondly, they smoothed the mean velocity profile and suppressed turbulence generated at the current inlet.

Four resistance-type wave probes were deployed in the present test programme. One was mounted at a permanent location 9 m from the mean flow inlet and provided a fixed frame of reference in the Fourier analysis. The other three probes were mounted on a rigid frame with spacings of 0.4 and 0.2 m between them. This frame was traversed along the flume to nine different locations, in steps of 0.1 m for the high frequency waves, and in steps of 0.2 m for the longer waves. This provided independent data for wave amplitude and phase at more than 20 different points along the flume. A multi-channel data acquisition system was used to record the output from the four wave monitors.

Each data record included a minimum of 50 wave periods and was sampled at 50 Hz. Ensemble averaging was performed relative to the fixed wave probe at $x = 9$ m, and the results decomposed by Fourier analysis to yield the amplitude and phase for each harmonic component. Procedures for data acquisition and analysis are summarised in Appendix A.

4. Recovering wavelengths

Before wavelengths can be calculated using the method described above, it is necessary to determine the incident wave amplitude and the reflection coefficient. Preliminary estimates were found by plotting the first harmonic wave amplitude against location along the flume and calculating the mean value and the amplitude of modula-

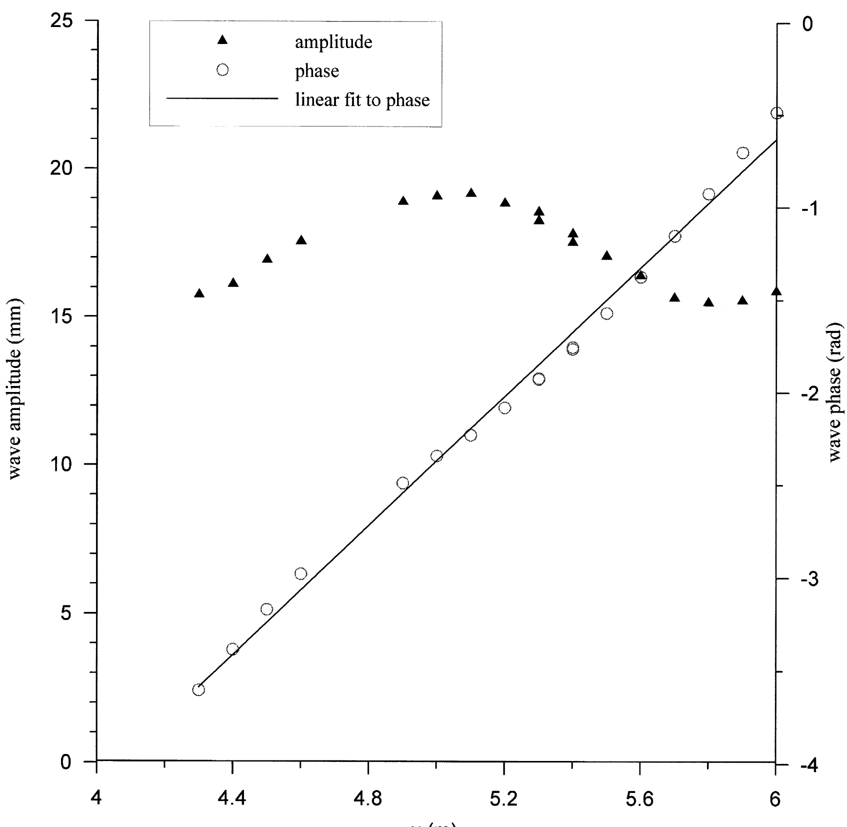

Fig. 5. Wave amplitude and phase along the flume: $T = 1.778$ s (17wf030), $h = 0.4$ m, following current.

tion, using data over at least one incident wavelength to allow an assessment of frictional wave attenuation.

The average rate of change of wave phase over a modulation length $L_R = L_1 L_2/(L_1 + L_2)$ is calculated iteratively. The procedure adopted here started with an estimate for the rate of change of phase derived from a least-squares linear fit through the full set of phase data. This was used with Eqs. (11) and (12) to determine the wavelength of the reflected wave, and hence, the modulation length over which the averaging had to be performed. (L_R could also be obtained directly from the graph of wave amplitude if attenuation was negligible and the data was not scattered.) The initial least-squares fit through the full set of phase data was then used as a base line against which to re-plot the same data points. If the resulting curve was not periodic about the base line over the estimated modulation length L_R, the slope of the base line was adjusted, the corresponding wavelength calculated, L_R adjusted accordingly, and the procedure repeated until satisfactory agreement was reached (Figs. 5 and 6). Because of the assumption of a linear Doppler shift when calculating the wavelength of the reflected wave, L_R was found to be relatively insensitive to adjustments in L_1, thus reducing one of the degrees

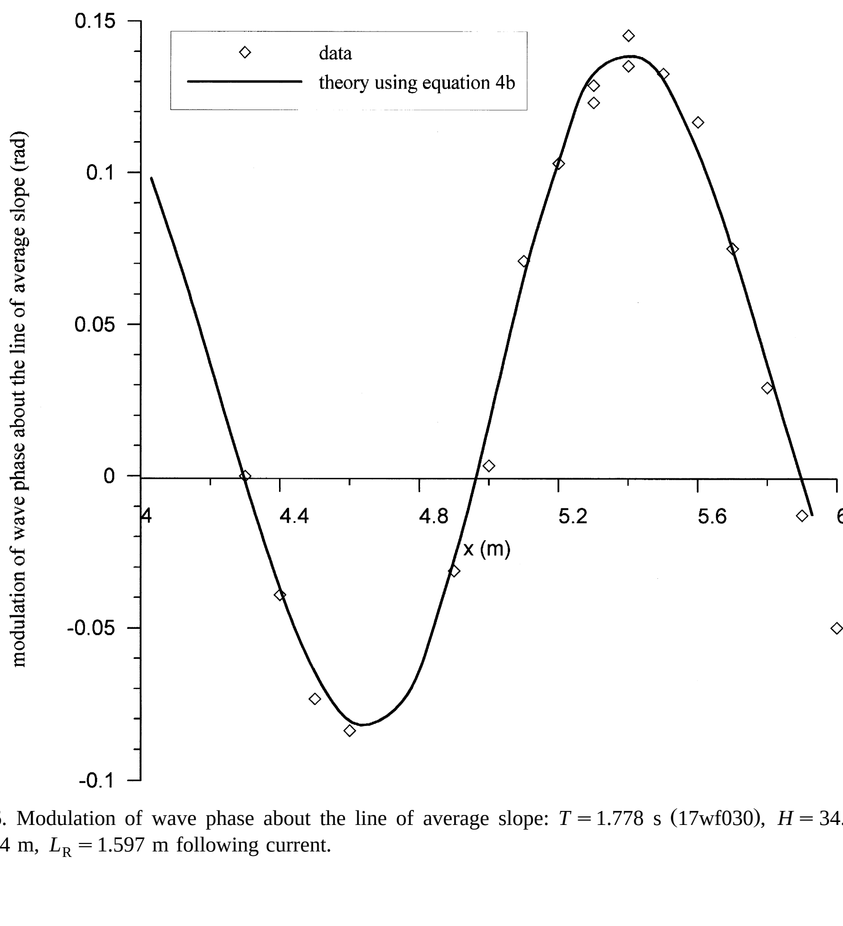

Fig. 6. Modulation of wave phase about the line of average slope: $T = 1.778$ s (17wf030), $H = 34.7$ mm, $h = 0.4$ m, $L_R = 1.597$ m following current.

Table 1
Experimental conditions and results for regular wave tests

Run code	Wave period, T (s)	Incident amplitude, a_1 (mm)	Reflection coefficient, α_r (%)	Modulation length, L_r (m)	Incident wavelength, L_1 (m)	Reflected wavelength, L_2 (m)	Effective current (m/s)	h/L_1
Regular waves								
Wave alone								
08wr015h	0.80	11.02	1.57	0.493	0.996	0.977	0.006	0.402
08wr030h	0.80	20.30	2.90	0.493	0.995	0.977	0.006	0.402
10wr015h	1.00	11.75	4.10	0.732	1.479	1.448	0.010	0.269
10wr030h	1.00	21.60	3.15	0.732	1.465	1.462	0.001	0.273
13wr030h	1.33	12.30	6.84	1.121	2.225	2.258	−0.009	0.180
14wr015h	1.42	12.89	3.00	1.220	2.398	2.485	−0.024	0.167
14wr030h	1.42	23.50	4.80	1.221	2.429	2.455	−0.007	0.165
14wr045h	1.42	34.30	2.00	1.221	2.456	2.424	0.008	0.163
17wr030h	1.78	20.20	6.40	1.628	3.229	3.214	0.004	0.127
20wr015h	2.00	14.55	1.20	1.847	3.660	3.729	−0.015	0.109
20wr030h	2.00	27.60	4.00	1.847	3.659	3.730	−0.016	0.109
25wr007h	2.50	9.10	5.10	2.369	4.730	4.748	−0.003	0.084
25wr021h	2.50	22.90	5.75	2.369	4.810	4.667	0.026	0.082
Following current								
08wf015h	0.80	8.80	3.10	0.460	1.187	0.752	0.142	0.337
08wf030h	0.80	18.20	3.00	0.464	1.177	0.766	0.135	0.340
10wf015h	1.00	8.80	6.00	0.702	1.692	1.200	0.148	0.236
10wf030h	1.00	17.90	5.00	0.704	1.684	1.210	0.143	0.237
13wf030h	1.33	10.00	9.93	1.100	2.490	1.972	0.143	0.161
14wf015h	1.42	10.30	8.00	1.204	2.687	2.180	0.136	0.149
14wf030h	1.42	19.50	6.40	1.203	2.690	2.177	0.138	0.149
14wf045h	1.42	30.30	5.80	1.202	2.696	2.170	0.141	0.148
17wf030h	1.78	17.35	11.00	1.597	3.480	2.953	0.125	0.115
20wf015h	2.00	12.10	14.60	1.802	4.020	3.359	0.144	0.100
20wf030h	2.00	22.10	16.50	1.802	4.030	3.348	0.149	0.100
25wf007h	2.50	7.50	20.00	2.351	5.130	4.275	0.145	0.078
25wf021h	2.50	20.50	17.70	2.351	5.130	4.340	0.145	0.078
Opposing current								
08wr015h	0.80	8.33	2.80	0.457	0.740	1.195	−0.148	0.541
08wr030h	0.80	17.10	2.40	0.461	0.754	1.185	−0.141	0.531
10wr015h	1.00	9.80	2.00	0.702	1.199	1.692	−0.148	0.334
10wr030h	1.00	19.30	3.50	0.703	1.206	1.687	−0.145	0.332
13wr030h	1.33	11.20	2.22	1.099	1.964	2.498	−0.147	0.204
14wr015h	1.42	11.65	16.00	1.200	2.190	2.678	−0.131	0.183
14wr030h	1.42	21.40	3.30	1.205	2.140	2.721	−0.156	0.187
14wr045h	1.42	32.20	1.50	1.202	2.171	2.695	−0.141	0.184
17wr030h	1.78	19.70	5.76	1.596	2.935	3.497	−0.133	0.136
20wr015h	2.00	13.90	4.00	1.828	3.339	4.038	−0.152	0.120
20wr030h	2.00	27.00	7.50	1.836	3.420	3.962	−0.118	0.117
25wr007h	2.50	8.33	9.90	2.349	4.320	5.149	−0.152	0.093
25wr021h	2.50	22.60	7.50	2.351	4.340	5.129	−0.144	0.092

of freedom in the procedure. Once the wavelengths were determined, it was possible to simulate the wave amplitude modulation along the flume using Eq. (4a). This gave the opportunity for further improvement in the estimates of incident and reflected wave amplitudes. PC-based spreadsheets were programmed to carry out all these calculations.

5. Results

Table 1 shows the results from the procedure described above, applied to waves covering a range through from deep-water to near shallow-water conditions. Three sets of tests were performed. Waves were generated initially with the current inlet and outlet closed, so that the only mean flow present was the weak mass transport induced by the waves themselves. A steady flow was then introduced along the flume and the full range of wave tests repeated, first with waves generated by the wave maker at the flow inlet end to produce data for the “following current” case, secondly with waves generated by the wave maker at the flow outlet end to produce “opposing current” data. In both cases, it was necessary to make minor adjustments to the outlet valve settings to maintain the same overall volume flow rate and mean depth for all tests.

Wavelengths measured for tests with waves alone were generally within 1.5% of those predicted by linear wave theory, equivalent to the addition of an effective mean flow of less than ± 0.025 m/s. Measurements made with a laser Doppler velocimeter (LDV) recorded mass transport velocities of the order of -0.015 m/s in the upper flow. This suggests that the technique for determining wavelength is accurate to well within a 1% error band, and that apparent discrepancies in wavelength measurements can be attributed largely to the effects of mean flows in the flume and to some of the wave conditions lying in a non-linear regime.

The effective current strengths deduced from wavelengths in the “following current” tests were surprisingly consistent around a value of 0.142 m/s. This compares with the

Table 2
Experimental conditions and results for bichromatic wave tests

Bichromatic: modulation period = 5.333 s	Wave period, T (s)	Incident amplitude, a_1 (mm)	Reflection coefficient, α_r (%)	Incident wavelength, L_1 (m)	Reflected wavelength, L_2 (m)	Effective current (m/s)	h/L_1
Wave alone							
Fourth harmonic	1.33	17.20	5.06	2.203	2.279	-0.021	0.182
Third harmonic	1.78	14.65	6.50	3.175	3.268	-0.022	0.126
Following current							
Fourth harmonic	1.33	14.40	7.50	2.498	1.963	0.148	0.160
Third harmonic	1.78	12.30	11.31	3.520	2.910	0.144	0.114
Opposing current							
Fourth harmonic	1.33	15.10	3.24	2.010	2.457	-0.123	0.199
Third harmonic	1.78	13.70	4.50	2.930	3.502	-0.135	0.137

mean current velocity outside the bottom boundary layer of 0.15 m/s observed using the LDV system. If Eq. (10) is used to predict wavelength using the near-surface mean velocity, implicitly assuming a uniform velocity profile through the depth, the error in predicted wavelength turns out to be less than 1%. Even better agreement is achieved by taking account of the non-uniform vertical distribution of mean velocity. This was

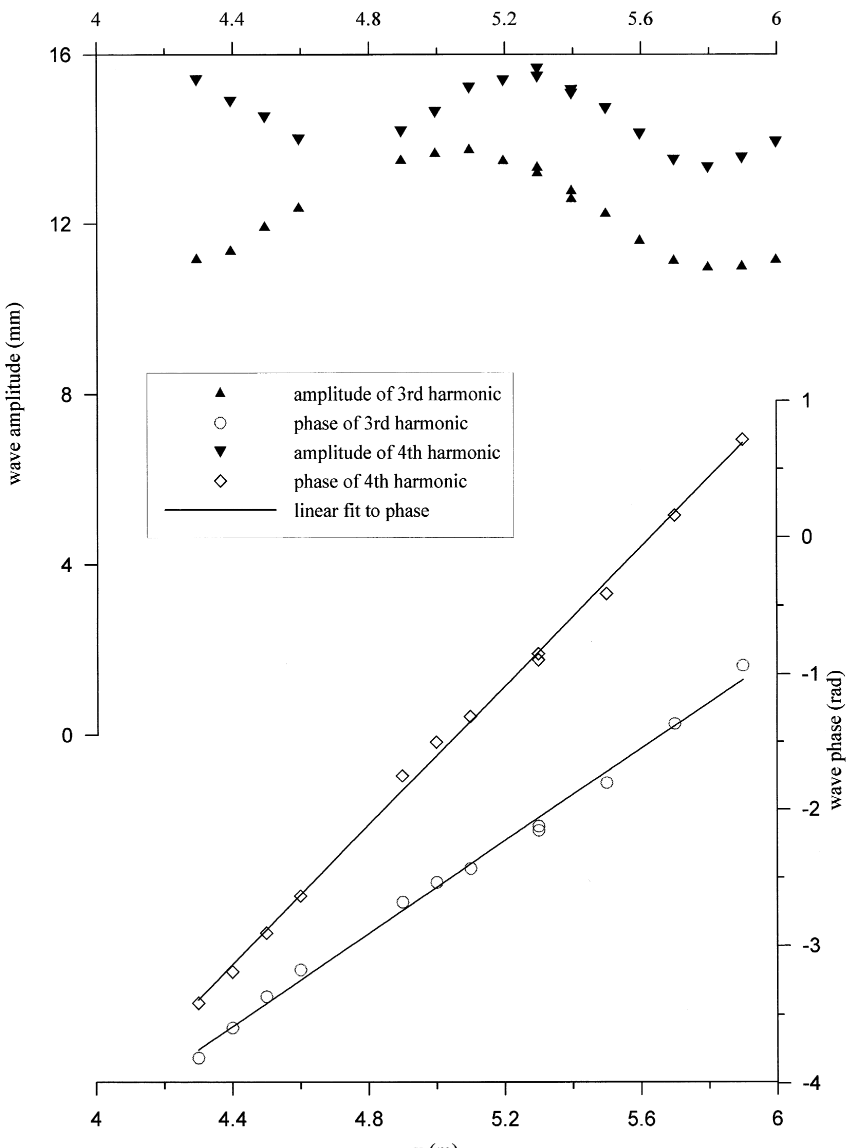

Fig. 7. Wave amplitude and phase along the flume for bichromatic wave: $T_3 = 1.778$ s and $T_4 = 1.333$ s, $h = 0.4$ m, following current.

achieved using the general formula for effective current for the case of a relatively weak mean flow proposed by Skop (1987):

$$c_a = \sqrt{\frac{g}{m}\tanh mh} + \frac{2m}{(1-e^{-4mh})}\left[\int_{-h}^{0} U(z)e^{2mz}dz + e^{-4mh}\int_{-h}^{0} U(z)e^{-2mz}dz\right] \tag{13}$$

where c_a is the absolute wave celerity, $U(z)$ describes the vertical mean current distribution, and z is the vertical coordinate measured upwards from still water level.

Results from the “opposing current” tests indicated a slightly higher effective mean current than for the following current, consistent with the wave mass transport inducing a reverse flow near the surface. There was, however, rather more scatter in the data. This was surprising in view of the low reflection coefficients.

A further series of tests was also performed using bichromatic waves with a modulation period of 5.33 s; results are shown in Table 2 for wave alone, following current, and opposing current. Again, the procedure was able to identify wavelengths of the two primary components and the effective current strength. Results were similar to those from the regular wave tests, Fig. 7.

Considering the reflection coefficients listed in Table 1, the most significant effect is the increase in α_r when the following current is superimposed. This can be attributed to the reduction in wave amplitude of the incident wave due to the stretching effect of the current, and to the steepening of the reflected wave by the same current. It may also relate to the sensitivity of the force-feedback absorption of the wave makers at low frequency in the presence of a current. However, the low reflection coefficients for all tests on waves alone show that the combination of active absorption and horizontal permeable beach provides a practical solution for the reduction of wave reflection over a wide range of wave and mean flow conditions.

6. Discussion

The procedure adopted in these tests depends on the flow conditions being steady and repeatable. In particular, it is essential that the mean current does not vary between sets of measurements for the same wave condition, either in flow rate or water depth. Using the four wave probes simultaneously, it was possible to measure the absolute wave phase at 21 locations along the flume with just seven repeats of the test. While in some situations this might be tedious, in the present application, these measurements were carried out at the same time that vertical profiles of velocity were being measured with the LDV.

It is also necessary to plan the experiment carefully so that the measurement positions along the flume span at least one half of an incident wavelength (ideally one or more full wavelengths). Twelve observations in half an incident wavelength were found to give good resolution, although the spacing between measurements could be increased if the test region extended over a greater length of the flume. Appendix A summarises the main steps required in this method.

The equation relating the local wave phase, ϕ, to wave amplitude and wave number (viz. Eq. (4b)) has been derived in a number of previous publications. However, the variation in $(d\phi/dx)$ in the direction of incident wave propagation, x, when a reflected wave is superimposed, implicit in Eq. (4b), has not been considered. Systematic differences in the "observed" wavelength dependent on the spacing and location of the wave probes, as illustrated in Fig. 8, have thus been overlooked. For example, for 2.5 s waves with a 5% reflection coefficient but no current superimposed, wavelengths calculated applying a two-probe method to different pairs of probe data spaced 2.0 m apart (equivalent to $0.45L_1$) are up to $\pm 1\%$ from their mean value. This error rises to

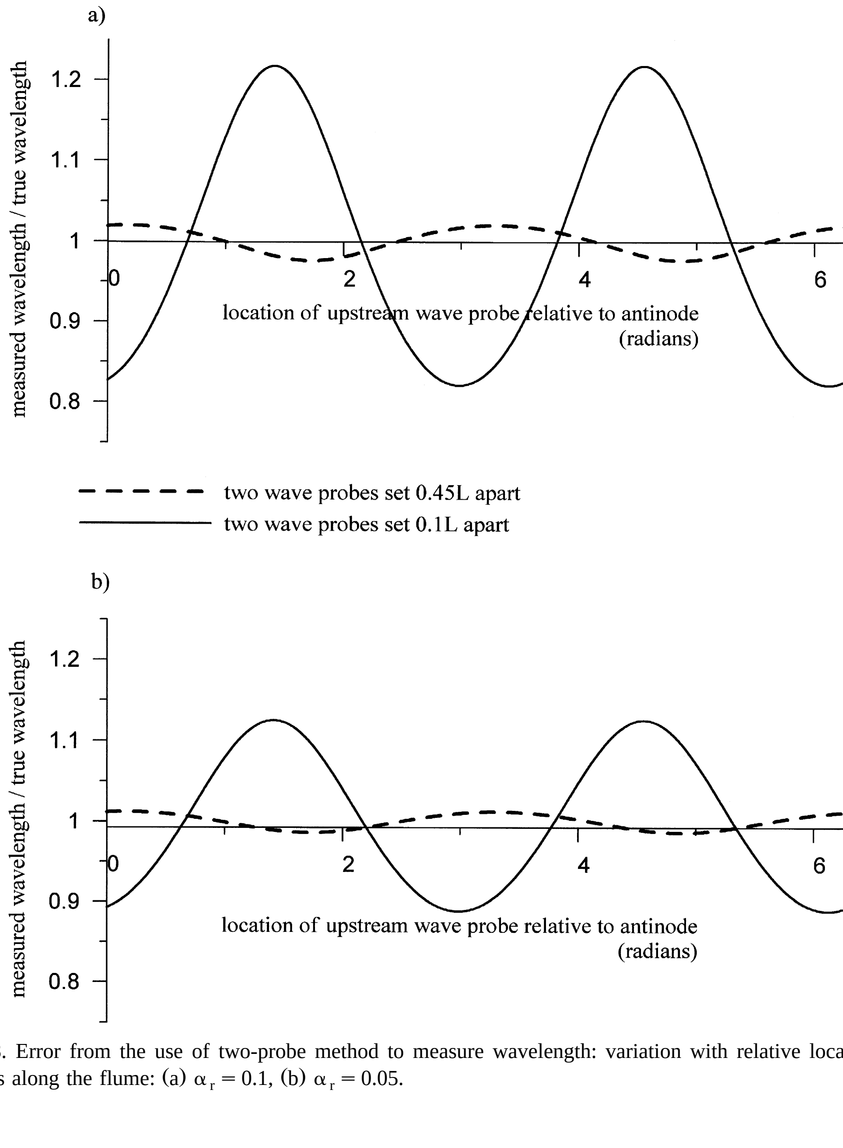

Fig. 8. Error from the use of two-probe method to measure wavelength: variation with relative location of probes along the flume: (a) $\alpha_r = 0.1$, (b) $\alpha_r = 0.05$.

between $\pm 12\%$ for sets of data spaced only 0.5 m apart (equivalent to $0.1 L_1$), as shown in Fig. 8b. For waves with reflection coefficients of 10% (Fig. 8a), the corresponding figures are $\pm 2\%$ and $\pm 20\%$, respectively. Clearly, the observed wavelength is sensitive both to the spacing between the two probes and also to their location along the flume relative to the partial standing wave pattern. The 5% discrepancy between wavelength observations and predictions from linear wave theory, and apparent sensitivity of reflection coefficients to wavelength reported by Cotter and Chakrabarti (1994) may stem from this effect.

In combined wave–current flows, other methods require an a priori knowledge of the mean current strength and its associated velocity profile in order to calculate the wavelength using the Doppler-shifted dispersion relation. It was noted above that this can lead to 1–2% errors for the present tests.

The spatial modulation of wave amplitude predicted in Eq. (4a) was confirmed in the present tests both with and without current superimposed. The distance between consecutive "quasi-antinodes" is thus *not* the half the incident wavelength but the modulation length $L_R = L_1 L_2 / (L_1 + L_2)$. However, even when a strong current is added and the reflection coefficient is small, L_R remains close to the equivalent wavelength in the absence of the current.

The present method has been shown to work for regular and bichromatic waves with a collinear current. Measurements have also been made of current-induced wave refraction in a 3-D wave basin. It can also be applied for experiments looking at the interaction of 2-D random waves with a mean current, and to the study of both free and bound higher harmonics.

7. Conclusions

Two-probe and three-probe methods published previously are able to correctly determine the wave reflection coefficients in a partial standing wave system with no current superimposed. However, if no account is taken of the spatial variation in wave phase slope in the direction of wave propagation caused by reflected waves, they cannot be used accurately to determine wavelength.

A method has been developed to calculate incident and reflected wavelengths and the effective current strength for laboratory waves with a non-uniform current superimposed. Results obtained using the method were within 1% of expected values. No prior knowledge was required of the mean flow.

Two absorbing wave makers, one at either end of the wave flume, used in conjunction with a horizontal perforated beach suspended below wave trough level, produced reflection coefficients between 1.2% and 6% for a wide range of wave conditions. This system is ideally suited to random wave tests.

Acknowledgements

This work was funded by the Commission of the European Communities Directorate General for Science, Research and Development under Contract MAS3-CT95-0011 as part of the KADWCI project: Kinematics and Dynamics of Wave–Current Interactions. The authors are grateful to Dr. Gareth Thomas (University College Cork, Eire) and Dr. Gert Klopman (Albatros Flow Research, The Netherlands) for their stimulating discussions on the subject of this paper.

Appendix A. Summary of the method to determine wavelength

A.1. Data sampling

Calibration	all wave probes should be calibrated at regular intervals
Duration	50 wave periods (minimum)
Synchronised	initiate data sample using wave generator software (or use signal from a wave probe at a fixed location in the test region)
Density	wave data from 24 different locations spaced evenly along the flume over one incident wavelength L_1 (calculated from first order theory in the absence of a current)

Extent of test region: to cover (at minimum) a span of $0.7L_1$ along the flume.

A.2. Processing

Fourier averaging of ensemble averaged data at each location along the flume to produce: amplitude A_x of the first harmonic, and phase of the first harmonic ϕ_x (relative to the same fixed time-base).

A.3. Analysis

Plot out amplitude A_x vs. location x along the flume, hence determine: a_1 from the mean value; a_2 from the amplitude of modulation; and L_r from the period of modulation.

Plot out phase ϕ_x vs. location x along the flume, hence determine: m_1 from the average slope over length L_r.

Construct a line of average slope passing through a single reference value for the phase.

Plot out the difference between the phase and the constructed line.

Check that the period of modulation is exactly L_r.

If not, adjust estimate of L_1, construct a new line of average slope through the same reference value of phase, re-plot the difference between the phase and the new constructed line to check if the period of modulation is now exactly L_R. Repeat until this is the case.

References

Cotter, D.C., Chakrabarti, S.K., 1994. Comparison of wave reflection equations with wave-tank data. J. Waterways, Port, Coastal, Ocean Eng. 120 (2), 226–232.

Goda, Y., Suzuki, Y., 1976. Estimation of incident and reflected waves in random wave experiments. Proc. 15th Int. Conf. Coastal Eng., 1, ASCE New York, 828–845.

Hughes, S.A., 1993. Laboratory wave reflection an analysis using co-located probes. Coastal Eng. 20, 223–237.

Kemp, P.H., Simons, R.R., 1983. The interaction of waves and a turbulent current: waves propagating against the current. J. Fluid Mech. 130, 73–89.

Klopman, G., 1994. Vertical structure of the flow due to waves and currents. Progress Report H840.30 Part ii. Delft Hydraulics, The Netherlands.

Mansard, E.P.D., Funke, E.R., 1980. The measurement of incident and reflected spectra using a least squares method. Proc. 17th Int. Conf. Coastal Eng., 1, ASCE New York, 154–172.

Seelig, W.N., 1979. Effect of breakwaters on waves: laboratory tests of wave transmission by overtopping. Proc. Coastal Struct. '79, ASCE New York, 941–961.

Skop, R.A., 1987. Approximate dispersion relation for wave–current interactions. J. Waterways, Port, Coastal Ocean Eng. 113, 187–195.

Skyner, D.J., Easson, W.J., 1998. Wave kinematics and surface parameters of steep waves travelling on sheared currents. J. Waterways, Port, Coastal, Ocean Eng. 124 (1), 1–6.

Thornton, E.B., Calhoun, R.J., 1972. Spectral resolution of breakwater reflected waves. J. Waterways, Harbour Coastal Eng., WW4 ASCE.

Zelt, J.A., Skjelbreia, J.E., 1992. Estimating incident and reflected wave fields using an arbitrary number of wave gauges. Proc. 23rd Int. Conf. Coastal Eng., ASCE New York, 777–789.